Alexandria Engineering Journal (2022) 61, 3037–3049

HOSTED BY

ELSEVIER

Alexandria University

Alexandria Engineering Journal

www.elsevier.com/locate/aej
www.sciencedirect.com

On a new method for finding numerical solutions to integro-differential equations based on Legendre multi-wavelets collocation

Imran Khan [a], Muhammad Asif [a], Rohul Amin [a], Qasem Al-Mdallal [b,*], Fahd Jarad [c,d,*]

[a] *Department of Mathematics, University of Peshawar, P. O. Box 25000, Khyber Pakhtunkhwa, Pakistan*
[b] *Department of Mathematical Sciences, UAE University, P. O. Box 15551, Al Ain, United Arab Emirates*
[c] *Department of Mathematics, Çankaya University, Etimesgut 06790, Ankara, Turkey*
[d] *Department of Medical Research, China Medical University, Taichung 40402, Taiwan*

Received 3 April 2021; revised 28 July 2021; accepted 13 August 2021
Available online 26 August 2021

KEYWORDS

Linear Legendre multi-wavelets;
Fredholm integro-differential equations of first and higher-orders;
Volterra integro-differential equations of first and higher-orders

Abstract In this article, a wavelet collocation method based on linear Legendre multi-wavelets is proposed for the numerical solution of the first as well as higher orders Fredholm, Volterra and Volterra–Fredholm integro-differential equations. The presented numerical method has the capability to tackle the solutions of both linear and nonlinear problems of these model equations. In order to endorse accuracy and efficiency of the method, it is tested on various numerical problems from literature with the aid of maximum absolute errors and rates of convergence. L_∞ norms are used to compare the numerical results with other available methods such as Multi-Scale-Galerkin's method, Haar wavelet collocation method and Meshless method from literature. The comparability of the presented method with other existing numerical methods demonstrates superior efficiency and accuracy.

1. Introduction

In the recent years, the solutions of integro-differential equations (IDEs) have gain great significance in various fields of science and engineering. The areas concerned are biology, chemistry, mechanics, physics, electrostatics, astronomy, economics, potential theory etc [14]. The IDEs are utilized to model most of the physical phenomena in simple mathematical formulations. These equations arise in fluid dynamics, biological models, chemical kinetic, ecology, control theory of finan-

* Corresponding authors at: Department of Mathematics, Çankaya University, Etimesgut 06790, Ankara, Turkey (F. Jarad).
E-mail addresses: lec.imranmath@uop.edu.pk (I. Khan), asif.tangi@uop.edu.pk (M. Asif), r.aminmath@uop.edu.pk (R. Amin), q.almdallal@uaeu.ac.ae (Q. Al-Mdallal), fahd@cankaya.edu.tr (F. Jarad).

Peer review under responsibility of Faculty of Engineering, Alexandria University.

https://doi.org/10.1016/j.aej.2021.08.032
1110-0168

cial mathematics, aerospace systems, industrial mathematics etc. More specific, the models which describes hereditary properties can model using IDEs. The analytical solution of the IDEs difficult and involve tedious calculations. Therefore, most the authors introduced numerical techniques for the solution of these types of equations.

In the last decades, the approximation theory regarding IDEs gained much popularity and many author developed numerical technique for the solution IDEs. Some the techniques are, Monotone iterative method [3,4], Meshless method [9], differential transform method [7], Bessel polynomial solution method [20], Tau method [10], finite difference method [22], rationalized Haar function method [13,24–26], Taylor collocation method [18], the CAS wavelet method [6], an improved Haar wavelet collocation method [16], homotopy perturbation method [19], spline-shooting method [2], Chebyshev collocation method [8], multiscale Galerkin method [5] and sine–cosine wavelet methods [11,12].

In the recent years, wavelets theory has played a significant role in signal processing. These wavelets are mainly scalar, where there is only one scaling function [32–34]. However, Linear Legendre multi-wavelets are based on more than one scaling function. Such growing interests in multiwavelets mainly stem from the following facts: linear Legendre multi-wavelets can simultaneously possess orthogonality, symmetry and a high order of approximation for a given support of the scaling functions (this is not possible for any real valued scaler wavelets) and secondly linear Legendre multiwavelets have produced promising results in the areas of image compression. A Linear Legendre multi-wavelets system can provide perfect reconstruction while preserving length (orthogonality), good performance at the boundaries (via linear-phase symmetry) and a high order of approximation (vanishing moments). Thus, Linear Legendre multi-wavelets offer the possibility of superior performance. Poisson equation is linear partial equation. The standard solution of the Poisson equation can also be derived in integral equation form [31].

Recently, many researcher utilized different basis functions *i.e*. wavelets and orthogonal functions to find out the approximate solution of IDEs. In various field of science and engineering wavelet basis are utilized to numerically approximate the solution of various problems. In literature, the Fredholm, Volterra and Fredholm–Volterra IDEs (both linear and nonlinear) are solved by utilizing different wavelets basis, in connection with different type of collocation techniques[16,21,13,6]. In this work, solution of IDEs is approximated with the help of family of linear Legendre multiwavelets.

In this article, three different types of IDEs of first and higher-order will be considered namely Fredholm IDEs, Volterra IDEs and Volterra–Fredholm IDEs. In the newly developed numerical technique all the cases comprises linear and nonlinear will be presented.

The article is designed in the subsequent manner. In Section 2, some definitions and a brief discussion on Legendre multi-wavelet are presented. In Section 3, the newly developed method is demonstrated. The efficiency and better performance of the method are given in Section 4, by testing it to some benchmark problems. Finally, conclusion of the study are presented in Section 5.

2. The linear Legendre multi-wavelets

The term wavelet means a small wave or simply an oscillation that decays decay rapidly is called a wavelet. The wavelets are piecewise continuous functions obtained from translation and dilation of main wavelet called the mother wavelet or mother function. The continuous change in translation parameter a and dilation parameter b result the formation of following continuous family of wavelets [27–30]:

$$v_{ab}(y) = \frac{v\left(\frac{1}{a}(y-b)\right)}{\sqrt{|a|}}, \quad a, b \in \mathbb{R}, a \neq 0. \tag{1}$$

Alternatively, the family of discrete wavelets is obtained when discrete values of the translation parameter $a = \frac{1}{2^l}$ and dilation parameter $b = \frac{n}{2^l}$ are utilized:

$$v_{ln}(y) = 2^{\frac{l}{2}} v(2^l y - n), \quad l, n \in \mathbb{Z}. \tag{2}$$

In addition to this, the mother function v will satisfy the equation $\int_{\mathbb{R}} v(y) = 0$.

In this work, the focus of the study is the discrete wavelets family. In particular case, in which an orthonormal basis of $L^2(\mathbb{R})$ are formed by the family of discrete wavelet, has various good properties. The multi-resolution analysis (MRA) will be utilized to get it, which is given below:

The sequence $\{V_l\}_{l\in\mathbb{Z}}$ which is increasing with scaling function $\chi \in V_0$ of closed subspaces of $L^2(\mathbb{R})$ is known as MRA if it satisfied the following conditions:

1. $\bigcup_l V_l$ is dense in $L^2(\mathbb{R})$ and $\bigcap_l V_l = \{0\}$,
2. $f(y) \in V_l$ iff $f(y/z^l) \in V_0$,
3. $\{\chi(y-n)\}_{n\in\mathbb{Z}}$ is a Riesz basis for V_0.

From condition 3, we can say that the sequence $\{2^l\chi(2^l y - n)\}_{n\in\mathbb{Z}}$ form an orthonormal basis for V_0. The author constructed linear LMWs in [15]. The scaling functions denoted by $\chi_0(y)$ and $\chi_1(y)$ are selected as under:

$$\chi_0(y) = 1 \text{ and } \chi_1(y) = \sqrt{3}(2y-1), \quad 0 \leqslant y < 1. \tag{3}$$

Then, the mother wavelet for the linear LMWs family is as follows:

$$v^0(y) = \begin{cases} -\sqrt{3}(4y-1) & \text{for } 0 \leqslant y < \frac{1}{2}, \\ \sqrt{3}(4y-3) & \text{for } \frac{1}{2} \leqslant y < 1, \end{cases} \tag{4}$$

and

$$v^1(y) = \begin{cases} (6y-1) & \text{for } 0 \leqslant y < \frac{1}{2}, \\ (6y-5) & \text{for } \frac{1}{2} \leqslant y < 1. \end{cases} \tag{5}$$

By the process of translation and dilation of the mother wavelet v we can easily obtained the linear LMWs and are given below:

$$\{v^k_{ln}(y) = 2^{l/2} v^k(2^l y - n), \quad l, n \in \mathbb{Z}, \quad k = 0, 1\}. \tag{6}$$

An orthonormal basis obtain from the family $\{v^k_{ln}\}^{k=0,1}_{l,n\in\mathbb{Z}}$ for $L^2(\mathbf{R})$ and from the subset $\{v^k_{ln}\}$ for $n = 0, 1, 2, 3, 4, \ldots, 2^l - 1, l = 0, 1, 2, 3, \ldots$and $k = 0, 1$ forms an orthonormal basis for $L^2[0, 1]$. Thus, any function $w(y) \in L^2[0, 1]$ is actually the linear combination of the family of linear LMWs as under:

$$w(y) = \lambda_0\, \chi_0(y) + \lambda_1\, \chi_1(y) + \sum_{l=0}^{\infty}\sum_{k=0}^{1}\sum_{n=0}^{2^l-1} \lambda_{ln}^k\, v_{ln}^k(y), \tag{7}$$

where

$$\lambda_{ln}^k = \langle g(y), v_{ln}^k \rangle, \tag{8}$$

and $\langle .,. \rangle$ is the inner product space. The series given above is truncated after finite terms to obtain an appropriate approximation, and it results

$$w(y) \approx \lambda_0\, \chi_0(y) + \lambda_1\, \chi_1(y) + \sum_{l=0}^{M}\sum_{k=0}^{1}\sum_{n=0}^{2^l-1} \lambda_{ln}^k\, v_{ln}^k(y). \tag{9}$$

Eq. (3) through Eq. (5) can be used to obtain the first four function χ_0, χ_1, v^0 and v^1. Furthermore, the next four functions are given bellow:

$$v_{10}^0(y) = \begin{cases} -\sqrt{6}(8y-1) & \text{for } 0 \leqslant y < \frac{1}{4}, \\ \sqrt{6}(8y-3) & \text{for } \frac{1}{4} \leqslant y < \frac{1}{2}, \\ 0 & \text{for } \frac{1}{2} \leqslant y < 1, \end{cases} \tag{10}$$

$$v_{11}^0(y) = \begin{cases} 0 & \text{for } 0 \leqslant y < \frac{1}{2}, \\ -\sqrt{6}(8y-5) & \text{for } \frac{1}{2} \leqslant y < \frac{3}{4}, \\ \sqrt{6}(8y-7) & \text{for } \frac{3}{4} \leqslant y < 1, \end{cases} \tag{11}$$

$$v_{10}^1(y) = \begin{cases} \sqrt{2}(12y-1) & \text{for } 0 \leqslant y < \frac{1}{4}, \\ \sqrt{2}(12y-5) & \text{for } \frac{1}{4} \leqslant y < \frac{1}{2}, \\ 0 & \text{for } \frac{1}{2} \leqslant y < 1, \end{cases} \tag{12}$$

and

$$v_{11}^1(y) = \begin{cases} 0 & \text{for } 0 \leqslant y < \frac{1}{2}, \\ \sqrt{2}(12y-7) & \text{for } \frac{1}{2} \leqslant y < \frac{3}{4}, \\ \sqrt{2}(12y-11) & \text{for } \frac{3}{4} \leqslant y < 1. \end{cases} \tag{13}$$

Other family members can be obtained using similar procedure.

As evident from the expression, the linear LMWs $\{v_{ln}^k : k = 0, 1,\ l, n \in \mathbb{Z}\}$, contains 3 parameters. In order to simplify the expression, the Linear LMWs $\{v_{ln}^k : k = 0, 1,\ l, n \in \mathbb{Z}\}$, is separated in sub wavelet families, which reduces the number of parameters to only one.

The notation $\{\alpha_j : j = 1, 2, \ldots\}$ which is the first family, is comprised of the first scaling function and mother wavelet generated wavalets $v^0(t)$. The below given representation is used for this subfamily:

$$\alpha_1(y) = 1, \quad 0 \leqslant y < 1, \tag{14}$$

and

$$\alpha_j(y) = \begin{cases} -2^{\frac{k}{2}}\sqrt{3}\left(2^{k+2}y - 4l - 1\right) & \text{for } \frac{l}{n} \leqslant y < \frac{l+\frac{1}{2}}{n}, \\ 2^{\frac{k}{2}}\sqrt{3}\left(2^{k+2}y - 4l - 3\right) & \text{for } \frac{l+\frac{1}{2}}{n} \leqslant y < \frac{l+1}{n}, \quad j = 2, 3, \ldots, \end{cases} \tag{15}$$

where, $l = 0, 1, \ldots, n-1$ and $n = 2^k$, $k = 0, 1, \ldots, K$. In the aforementioned k denotes the level of wavelet resolution and the maximum number of resolution is denoted by letter K. The translation parameter is expressed by letter l. The relation among the notations j, l and n can be defined as $j = l + n + 1$.

The second wavelets are of the form $\{\theta_j : j = 1, 2, \ldots\}$ and the remaining wavelets in the family are calculated from the mother wavelet $v^1(y)$. These can be written in the following alternate form:

$$\theta_1(y) = \sqrt{3}(2y-1), \quad 0 \leqslant y < 1, \tag{16}$$

and

$$\theta_j(y) = \begin{cases} 2^{\frac{k}{2}}\left(3 \times 2^{k+1}y - 6l - 1\right) & \text{for } \frac{l}{n} \leqslant y < \frac{l+\frac{1}{2}}{n}, \\ 2^{\frac{k}{2}}\left(3 \times 2^{k+1}y - 6l - 5\right) & \text{for } \frac{l+\frac{1}{2}}{n} \leqslant y < \frac{l+1}{n}, \quad j = 2, 3, \ldots, \end{cases} \tag{17}$$

where n, k and l can be defined in the same fashion as above.

Any function $w(y) \in L^2(a, b)$ in Eq. (7) can be formed from the linear combination of linear LMWs by utilizing the alternate formulation of these wavelets as under:

$$w(y) = \sum_{j=1}^{\infty} c_j \chi_j(y) + \sum_{j=1}^{\infty} d_j \varphi_j(y), \tag{18}$$

and the approximation for $w(y)$ given in Eq. (9) yield

$$w(y) \approx \sum_{j=1}^{\frac{1}{2}M} c_j \chi_j(y) + \sum_{j=1}^{\frac{1}{2}M} d_j \varphi_j(y). \tag{19}$$

In the similar manner the truncated expression for first and higher orders are given as under:

$$w\prime(y) \approx \sum_{j=1}^{\frac{1}{2}M} c_j \chi_j(y) + \sum_{j=1}^{\frac{1}{2}M} d_j \varphi_j(y), \tag{20}$$

$$w\prime\prime(y) \approx \sum_{j=1}^{\frac{1}{2}M} c_j \chi_j(y) + \sum_{j=1}^{\frac{1}{2}M} d_j \varphi_j(y), \tag{21}$$

$$w(y)^{iv} \approx \sum_{j=1}^{\frac{1}{2}M} c_j \chi_j(y) + \sum_{j=1}^{\frac{1}{2}M} d_j \varphi_j(y), \tag{22}$$

where $M = 2^{k+2}, c_j$, are called the LMWs coefficients and d_j where $j = 1, 2, \ldots, \frac{1}{2}M$ are the unknown coefficients of linear LMWs.

3. Numerical procedure

In this section, quadrature technique with linear LMWs basis is applied for numerical integration, followed by the detailed explanation of the presented method based on linear LMWs for various kinds of integro-differential equations comprising Fredholm IDEs and Volterra IDEs of the first and higher order individually. The following discrete points are used for linear LMWs approximations:

$$y_k = \frac{k - \frac{1}{2}}{M}, \; k = 1, 2, \ldots, M. \tag{23}$$

The quadrature rule for numerical integration by utilizing linear LMWs on the close interval $[0, 1]$ is as follows:

$$\int_0^1 f(y)\, dy = \frac{1}{M}\sum_{k=1}^{M} f(y_k). \tag{24}$$

Generally, for any interval $[c, d]$ given in [1], we have

$$\int_c^d f(y)\,dy = \frac{(d-c)}{M}\int_0^1 f(c-(c-d)t)\,dt = \frac{(d-c)}{M}\sum_{l=1}^{M} f(t_l), \tag{25}$$

where

$$t_l = c + (d-c)\left(\frac{l-\frac{1}{2}}{M}\right), l = 1,2,\ldots,M. \tag{26}$$

3.1. Fredholm IDEs

In this portion of the section the presented technique will be considered for linear and nonlinear Fredholm IDEs of the first- and higher-orders.

3.1.1. First-order Fredholm IDEs

3.1.1.1. linear case. Let us take the subsequent linear Fredholm IDEs of the first order:

$$w\prime(y) + w(y)h(y) = f(y) + \int_0^1 w(\tau)K(y,\tau)\mathrm{d}\tau, w(0) = w_0. \tag{27}$$

Integrating Eq. (20) and utilizing the initial condition $w(0) = w_0$, we obtained the unknown function $w(y)$.

$$w(y) = u_0 + \sum_{j=1}^{\frac{1}{2}M} c_j\chi_j^1(y) + \sum_{j=1}^{\frac{1}{2}M} d_j\varphi_j^1(y), \tag{28}$$

where

$$\chi_j^1(y) = \int_0^y \chi_j(y)\mathrm{d}\tau, \varphi_j^1(y) = \int_0^y \varphi_j(y)\mathrm{d}\tau. \tag{29}$$

Now utilizing integration rule as defined in Eq. (25), the Eq. (27) gives:

$$w\prime(y) + h(y)w(y) = f(y) + \frac{1}{M}\sum_{k=1}^{M} K(y,\tau_l)w(\tau_l). \tag{30}$$

By substituting the approximate expressions for $w\prime(y)$, $w(y)$ given in Eqs. (20), (28)discretizing we obtained:

$$\sum_{j=1}^{\frac{1}{2}M} c_j\chi_j(y_k) + \sum_{j=1}^{\frac{1}{2}M} d_j\varphi_j(y_k) + h(y_k)\left(u_0 + \sum_{j=1}^{\frac{1}{2}M} c_j\chi_j^1(y_k) + \sum_{j=1}^{\frac{1}{2}M} d_j\varphi_j^1(y_k)\right) = f(y_k) + \frac{1}{N}\sum_{k=1}^{N} K(y_k,\tau_l)\left(u_0 + \sum_{j=1}^{\frac{1}{2}M} c_j\chi_j^1(\tau_l) + \sum_{j=1}^{\frac{1}{2}M} d_j\varphi_j^1(\tau_l)\right), j = 1,2,\ldots,M. \tag{31}$$

By simplifying the above equation, we get the following form:

$$\sum_{j=1}^{\frac{1}{2}M} c_j\left(\chi_j(y_k) - \frac{1}{M}\sum_{k=1}^{M} K(y_k,\tau_l)\chi_j^1(\tau_l)\right) + \sum_{j=1}^{\frac{1}{2}M} d_j\left(\varphi_j(y_k) - \frac{1}{M}\sum_{k=1}^{M} K(y_k,\tau_l)\varphi_j^1(\tau_l)\right) = f(y_k) - h(y_k)w_0 + \frac{1}{M}\sum_{k=1}^{M} K(y_k,\tau_l)w_0, \quad j = 1,2,\ldots,N. \tag{32}$$

Eq. (32) produces an $M \times M$ system of linear equations with unknowns $c_j, j = 1,2,\ldots,\frac{1}{2}M$ and $d_j, j = 1,2,\ldots,\frac{1}{2}M$. The system can be solved for the unknowns by using any linear technique. These unknowns are then used in Eq. (19) to approximate the solution of the Fredholm IDEs at collocation points y_k, $k = 1,2,\ldots,M$.

3.1.1.2. Nonlinear case. Consider the following first-order nonlinear Fredholm IDE:

$$w\prime(y) + h(y)w(y) = f(y) + \int_0^1 K(y,\tau,w(\tau))\mathrm{d}\tau, w(0) = w_0. \tag{33}$$

Applying technique of integration we get the following form:

$$w\prime(y) + h(y)w(y) = f(y) + \frac{1}{M}\sum_{k=1}^{M} K(y,\tau_l,w(\tau_l)). \tag{34}$$

Now putting the approximate expressions for $w(y)$ and $w\prime(y)$ in terms of truncated linear LMWs and discretizing.

$$Q_j\quad (c_1,c_2,\ldots,c_{\frac{M}{2}},d_1,d_2,\ldots,d_{\frac{M}{2}}) = \sum_{j=1}^{\frac{1}{2}M} c_j\chi_j(y_k) + \sum_{j=1}^{\frac{1}{2}M} d_j\varphi_j(y_k) + h(y_k)\left(u_0 + \sum_{j=1}^{\frac{1}{2}M} c_j\chi_j^1(y_k) + \sum_{j=1}^{\frac{1}{2}M} d_j\varphi_j^1(y_k)\right) - \frac{1}{M}\sum_{k=1}^{M} K\left(y_k,\tau_l,u_0 + \sum_{j=1}^{\frac{1}{2}M} c_j\chi_j^1(\tau_l) + \sum_{j=1}^{\frac{1}{2}M} d_j\varphi_j^1(\tau_l)\right) - f(y_k) = 0, j = 1,2,\ldots,M. \tag{35}$$

The above equation represents $M \times M$ system of nonlinear equations with unknowns $c_j, j = 1,2,\ldots,\frac{1}{2}M$ and $d_j, j = 1,2,\ldots,\frac{1}{2}M$. In order to compute the unknowns, **Newton's** or **Broyden's** techniques can be applied. Finally, the numerical solution can be obtained utilizing these unknown coefficients.

The Jacobian for **Newton's** or **Broyden's** is calculated using the following partial derivatives.

$$\frac{\partial Q_j}{\partial c_m} = \chi_m(y_k) + h(y_k)\chi_m^1(y_k) - \frac{1}{N}\sum_{k=1}^{N}\frac{\partial K}{\partial w}\chi_m^1(\tau_l), \quad j = 1,2,\ldots,M, \tag{36}$$

and

$$\frac{\partial Q_j}{\partial d_m} = \varphi_m(y_k) + h(y_k)\varphi_m^1(y_k) - \frac{1}{N}\sum_{k=1}^{N}\frac{\partial K}{\partial w}\varphi_m^1(\tau_l), \quad j = 1,2,\ldots,M. \tag{37}$$

3.1.2. Second-order boundary-value Fredholm IDEs

3.1.2.1. linear case. Consider the subsequent second-order linear FIDE:

$$w\prime\prime(y) + h_1(y)w\prime(y) + h(y)w(y) = f(y) + \int_0^1 w(\tau)K(y,\tau)\mathrm{d}\tau, w(0) = w_0, w(1) = w_1. \tag{38}$$

By using technique of integration for Eq. (21) and using the boundary conditions, we will get the approximate expressions for $w\prime(y)$ and $w(y)$ in the subsequent forms:

$$w\prime(y) = w_1 - w_0 - \sum_{j=1}^{\frac{1}{2}M} c_jc_1 - \sum_{j=1}^{\frac{1}{2}M} d_jd_1 + \sum_{j=1}^{\frac{1}{2}M} c_j\chi_j^1(y) + \sum_{j=1}^{\frac{1}{2}M} d_j\varphi_j^1(y), \tag{39}$$

and

$$w(y) = u_0 + x\left(w_1 - w_0 - \sum_{j=1}^{\frac{1}{2}M} c_j c_1 - \sum_{j=1}^{\frac{1}{2}M} d_i d_1\right) + \sum_{j=1}^{\frac{1}{2}M} c_i \chi_j^2(y) + \sum_{j=1}^{\frac{1}{2}M} d_j \varphi_j^2(y), \tag{40}$$

where

$$\chi_j^2(y) = \int_0^y \chi_j^1(y)\mathrm{d}\tau, \varphi_j^2(y) = \int_0^y \varphi_j^1(y)\mathrm{d}\tau, \tag{41}$$

and

$$\alpha_1 = \int_0^1 \chi_j^1(y)\mathrm{d}\tau, \beta_1 = \int_0^1 \varphi_j^1(y)\mathrm{d}\tau. \tag{42}$$

Now utilizing the integration rule as described in Eq. (25) for the aforementioned Eq. (38), we have:

$$w''(y) + h_1(y)w'(y) + h(y)w(y) = f(y) + \frac{1}{M}\sum_{k=1}^{M} w(\tau_k)K(y, \tau_k). \tag{43}$$

Now replacing $w''(y)$, $w'(y)$ and $w(y)$ by their respective approximate expressions as derived in Eqs. (21), (39) and (40)then discretizing the domain, we get the subsequent system of linear equations:

$$\begin{aligned}
&\sum_{j=1}^{\frac{1}{2}M} c_j\chi_j(y_k) + \sum_{j=1}^{\frac{1}{2}M} d_j\varphi_j(y_k) + h_1(y_k)\left(w_1 - w_0 - \sum_{j=1}^{\frac{1}{2}M} c_j\alpha_1 - \sum_{j=1}^{\frac{1}{2}M} d_j\beta_1 + \sum_{j=1}^{\frac{1}{2}M} c_j\chi_j^1(y_k)\right.\\
&\left.+\sum_{j=1}^{\frac{1}{2}M} d_j\varphi_j^1(y_k)\right) + h(y_k)\left(w_0 + y_k\left(w_1 - w_0 - \sum_{j=1}^{\frac{1}{2}M} c_j\alpha_1 - \sum_{j=1}^{\frac{1}{2}M} d_j\beta_1\right) + \sum_{j=1}^{\frac{1}{2}M} c_j\chi_j^2(y_k)\right.\\
&\left.+\sum_{j=1}^{\frac{1}{2}M} d_j\varphi_j^2(y_k)\right) = f(y_k) + \frac{1}{M}\sum_{j=1}^{M} K(y_k, \tau_k)\left(w_0 + \tau_k\left(w_1 - w_0 - \sum_{j=1}^{\frac{1}{2}M} c_j\alpha_1 - \sum_{j=1}^{\frac{1}{2}M} d_j\beta_1\right)\right.\\
&\left.+\sum_{j=1}^{\frac{1}{2}M} c_j\chi_j^2(\tau_k) + \sum_{j=1}^{\frac{1}{2}M} d_j\varphi_j^2(\tau_k)\right), j = 1, 2, \ldots, M.
\end{aligned} \tag{44}$$

The simplified form of the above Eq. (44) is as under:

$$\begin{aligned}
&\sum_{j=1}^{\frac{1}{2}M} c_j\left(\chi_j(y_k) + h_1(y_k)(\alpha_1 + \chi_j^1(y_k)) + h(y_k)(-y_k\alpha_1 + \chi_j^2(y_k)) - \frac{1}{M}\sum_{j=1}^{M} K(y_k, \tau_k)(-\tau_k\alpha_1\right.\\
&\left.+\chi_j^2(\tau_k))\right) + \sum_{j=1}^{\frac{1}{2}M} d_j\left(\varphi_j(y_k) + h_1(y_k)(\beta_1 + \varphi_j^1(y_k)) + h(y_k)(-y_k\beta_1 + \varphi_j^2(y_k))\right.\\
&\left.-\frac{1}{M}\sum_{j=1}^{M} K(y_k, \tau_k)(-\tau_k\beta_1 + \varphi_j^2(\tau_k))\right) = f(y_k) + h_1(y_k)(w_0 - w_1) + h(y_k)(y_k(w_0 - w_1) - w_0)\\
&+\frac{1}{M}\sum_{j=1}^{M} K(y_k, \tau_k)(w_0 + \tau_k(w_1 - w_0)),\ j = 1, 2, \ldots, M.
\end{aligned} \tag{45}$$

The approximate solution of the above equation is obtained by the procedure adopted for first-order linear Fredholm IDEs in the previous section.

3.1.2.2. Nonlinear case. Consider the subsequent 1^{st}-order nonlinear Fredholm IDE:

$$w''(y) + h_1(y)w'(y) + h(y)w(y) = f(y) + \int_0^1 K(y, \tau, w(\tau))\mathrm{d}\tau, w(0) = w_0, w(1) = w_1. \tag{46}$$

Integration and utilizing the boundary conditions we get:

$$w''(y) + h_1(y)w'(y) + h(y)w(y) = f(y) + \frac{1}{M}\sum_{k=1}^{M} K(y, \tau_k, w(\tau_k)). \tag{47}$$

Replacing $w(y), w'(y)$ and $w''(y)$ by its approximate linear Legendre wavelets values and discretizing, it follows

$$\begin{aligned}
&Q_j\ (\alpha_1, c_2, \ldots, c_{\frac{M}{2}}, \beta_1, d_2, \ldots, d_{\frac{M}{2}})\\
&= \sum_{k=1}^{\frac{1}{2}M} c_j\chi_j(y_k) + \sum_{j=1}^{\frac{1}{2}M} d_j\varphi_j(y_k) + h_1(y_k)\left(w_1 - w_0 - \sum_{j=1}^{\frac{1}{2}M} c_j\alpha_1 - \sum_{j=1}^{\frac{1}{2}M} d_j\beta_1 + \sum_{j=1}^{\frac{1}{2}M} c_j\chi_j^1(y_k)\right.\\
&\left.+\sum_{j=1}^{\frac{1}{2}M} d_j\varphi_j^1(y_k)\right) + h(y_k)\left(w_0 + y_k\left(w_1 - w_0 - \sum_{j=1}^{\frac{1}{2}M} c_j\alpha_1 - \sum_{j=1}^{\frac{1}{2}M} d_j\beta_1\right) + \sum_{j=1}^{\frac{1}{2}M} c_j\chi_j^2(y_k)\right.\\
&\left.+\sum_{j=1}^{\frac{1}{2}M} d_j\varphi_j^2(y_k)\right) - \frac{1}{N}\sum_{k=1}^{N} K\left(y_k, \tau_k, w_0 + \tau_k\left(w_1 - w_0 - \sum_{j=1}^{\frac{1}{2}M} c_j\alpha_1 - \sum_{j=1}^{\frac{1}{2}M} d_j\beta_1\right)\right.\\
&\left.+\sum_{j=1}^{\frac{1}{2}M} c_j\chi_j^2(\tau_k) + \sum_{j=1}^{\frac{1}{2}M} d_j\varphi_j^2(\tau_k)\right) - f(y_k) = 0, k = 1, 2, \ldots, N.
\end{aligned} \tag{48}$$

The above system will be solved by the same procedure as explained in case of 1^{st} order nonlinear Fredholm IDEs

The Jacobian of the system of equations provided in Eq. (48) can be computed using their subsequent derivatives.

$$\begin{aligned}
\frac{\partial Q_j}{\partial c_m} = \quad &\chi_m(y_k) + h_1(y_k)(-\alpha_1(m) + \phi_m^1(y_k)) + h(y_k)(-y_k\alpha_1(m) + \chi_m^2(y_k))\\
&-\frac{1}{M}\sum_{k=1}^{M} \frac{\partial K}{\partial w}(\tau_k\alpha_1(m) + \chi_m^2(\tau_k)), \quad k = 1, 2, \ldots, N,
\end{aligned} \tag{49}$$

and

$$\begin{aligned}
\frac{\partial Q_j}{\partial d_m} = \quad &\varphi_m(y_k) + h_1(y_k)(-\beta_1(m) + \varphi_m^1(y_k)) + h(y_k)(-y_k\beta_1(m) + \varphi_m^2(y_k))\\
&-\frac{1}{M}\sum_{k=1}^{M} \frac{\partial K}{\partial w}(\tau_k\beta_1(m) + \varphi_m^2(\tau_k)), \quad k = 1, 2, \ldots, M.
\end{aligned} \tag{50}$$

3.2. Volterra IDEs

In this portion the newly established numerical technique will be utilized for linear and nonlinear Volterra IDEs with 1^{st} and higher-orders.

3.2.1. $\mathbf{1^{st}}$*-order Volterra IDEs*

3.2.1.1. linear case. Consider the following 1^{st}-order linear Volterra IDE:

$$w'(y) + h(y)w(y) = f(y) + \int_0^y w(\tau)K(y, \tau)\mathrm{d}\tau, w(0) = w_0. \tag{51}$$

To obtained $w(y)$, integrate Eq. (20) and using the initial condition $w(0) = w_0$, we get:

$$w(y) = w_0 + \sum_{j=1}^{\frac{1}{2}M} c_j\chi_j^1(y) + \sum_{j=1}^{\frac{1}{2}M} d_j\varphi_j^1(y), \tag{52}$$

where

$$\chi_j^1(y) = \int_0^y \chi_j(y)\mathrm{d}\tau, \tag{53}$$

and

$$\varphi_j^1(y) = \int_0^y \varphi_j(y)\mathrm{d}\tau. \tag{54}$$

Applying the numerical integration formula in Eq. (25) through Eq. (51), we get:

$$w\prime(y)+h(y)\,w(y)=f(y)+\frac{y_j}{M}\sum_{k=1}^{N}w(\tau_k)\,K(y,\tau_k). \tag{55}$$

Now first substitute the approximate values of $w\prime(y)$, $w(y)$ given in Eqs. (20), (52) then the collocation points defined in Eq. (23) into the Eq. (55), we get

$$\sum_{i=1}^{\frac{1}{2}M}c_i\chi_i(y_j)+\sum_{i=1}^{\frac{1}{2}M}d_i\phi_i(y_j)+h(y_j)\left(w_0+\sum_{i=1}^{\frac{1}{2}M}c_i\chi_i^1(y_j)+\sum_{i=1}^{\frac{1}{2}M}d_i\phi_i^1(y_j)\right)=f(y_j)$$
$$+\frac{y_j}{N}\sum_{k=1}^{M}K(y_j,\tau_k)\left(w_0+\sum_{i=1}^{\frac{1}{2}M}c_i\chi_i^1(\tau_k)+\sum_{i=1}^{\frac{1}{2}M}d_i\phi_i^1(\tau_k)\right),k=1,2,\ldots,M. \tag{56}$$

After simplification Eq. (56) becomes:

$$\sum_{i=1}^{\frac{1}{2}M}c_i\left(\chi_i(y_j)-\frac{y_j}{M}\sum_{k=1}^{M}K(y_j,\tau_k)\,\chi_i^1(\tau_k)\right)+\sum_{i=1}^{\frac{1}{2}M}d_i\left(\phi_i(y_j)-\frac{x_j}{M}\sum_{k=1}^{M}K(y_j,\tau_k)\,\phi_i^1(\tau_k)\right)$$
$$=f(y_j)-h(y_j)\,w_0+\frac{y_j}{M}\sum_{k=1}^{M}K(y_j,\tau_k)\,w_0,\quad k=1,2,\ldots,M. \tag{57}$$

The same procedure, as discussed above in the linear cases of first-order Fredholm and Volterra IDEs, can be used to obtain the numerical solution.

3.2.1.2. Nonlinear case. The following first-order nonlinear Volterra integro-differential equation is considered:

$$w\prime(y)+h(y)\,w(y)=f(y)+\int_0^y K(y,\tau,w(\tau))\,d\tau,w(0)=w_0. \tag{58}$$

Numerical integration yields the following equation:

$$w\prime(y)+w(y)\,h(y)=f(y)+\frac{y_j}{M}\sum_{k=1}^{M}K(y,\tau_k,w(\tau_k)). \tag{59}$$

Approximating $w(y)$ and $w\prime(y)$ by its linear Legendre wavelets expression, the following equation is obtained after discretization

$$Q_j\ (c_1,c_2,\ldots,c_{\frac{M}{2}},d_1,d_2,\ldots,d_{\frac{M}{2}})$$
$$=\sum_{i=1}^{\frac{1}{2}M}a_i\chi_i(y_j)+\sum_{i=1}^{\frac{1}{2}M}d_i\phi_i(y_j)+h(y_j)\left(w_0+\sum_{i=1}^{\frac{1}{2}M}c_i\chi_i^1(y_j)+\sum_{i=1}^{\frac{1}{2}M}d_i\phi_i^1(y_j)\right)$$
$$-\frac{y_j}{M}\sum_{k=1}^{M}K\left(y_j,\tau_k,w_0+\sum_{i=1}^{\frac{1}{2}M}c_i\chi_i^1(\tau_k)+\sum_{i=1}^{\frac{1}{2}M}d_i\phi_i^1(\tau_k)\right)-f(y_j)=0,j=1,2,\ldots,M. \tag{60}$$

The remaining procedure is same as the one discussed in the nonlinear cases of Fredholm and Volterra IDEs.

The Jaccobian of the system given in Eq. (60) is computed with the help of the following partial derivatives.

$$\frac{\partial Q_j}{\partial c_m}=\chi_m(y_j)+h(y_j)\,\chi_m^1(y_j)-\frac{y_j}{M}\sum_{k=1}^{M}\frac{\partial K}{\partial w}\,\chi_m^1(\tau_k),\quad j=1,2,\ldots,M, \tag{61}$$

and

$$\frac{\partial Q_j}{\partial b_m}=\phi_m(y_j)+h(y_j)\,\phi_m^1(y_j)-\frac{y_j}{M}\sum_{k=1}^{M}\frac{\partial K}{\partial w}\,\phi_m^1(\tau_k),\quad j=1,2,\ldots,M. \tag{62}$$

3.2.2. Second-order initial-value Volterra IDEs

3.2.2.1. linear case. In this subsection we take the bellow given second-order linear Volterra IDEs:

$$w\prime\prime(y)+h_1(y)\,w\prime(y)+h(y)\,u(y)$$
$$=f(y)+\int_0^y w(\tau)\,K(y,\tau)\mathrm{d}\tau,w(0)=w_0,w\prime(0)=w\prime_0. \tag{63}$$

To obtained $w\prime(y)$ and $w(y)$, integrate Eq. (21) and using the boundary conditions $w(0)=w_0, w(0)=w\prime_0$, we get:

$$w\prime(y)=w\prime_0+\sum_{i=1}^{\frac{1}{2}M}c_i\chi_i^1(y)+\sum_{i=1}^{\frac{1}{2}M}d_i\phi_i^1(y), \tag{64}$$

and

$$w(y)=w_0+yw\prime_0+\sum_{i=1}^{\frac{1}{2}M}a_i\chi_i^2(y)+\sum_{i=1}^{\frac{1}{2}M}d_i\phi_i^2(y), \tag{65}$$

where

$$\chi_i^2(y)=\int_0^y\chi_i^1(y)\mathrm{d}\tau,\phi_i^2(y)=\int_0^y\phi_i^1(y)\mathrm{d}\tau, \tag{66}$$

$$c_1=\int_0^1\chi_i^1(y)\mathrm{d}\tau, \tag{67}$$

and

$$d_1=\int_0^1\phi_i^1(y)\mathrm{d}\tau. \tag{68}$$

Applying the formula of numerical integration on Eqs. (25)–(63), we get:

$$w\prime\prime(y)+h_1(y)\,w\prime(y)+h(y)\,w(y)$$
$$=f(y)+\frac{1}{N}\sum_{k=1}^{M}K(y,\tau_k)\,w(\tau_k). \tag{69}$$

Now first using the approximations of $w\prime\prime(y)$, $w\prime(y)$ and $w(y)$ given in Eqs. (21), (64) and (65)then the collocation points given in Eq. (23) into the equation given above, it follows:

$$\sum_{i=1}^{\frac{1}{2}M}c_i\chi_i(y_j)+\sum_{i=1}^{\frac{1}{2}M}M_i\phi_i(y_j)+h_1(y_j)\left(w\prime_0+\sum_{i=1}^{\frac{1}{2}M}a_i\chi_i^1(y_j)+\sum_{i=1}^{\frac{1}{2}M}b_i\phi_i^1(y_j)\right)$$
$$+h(y_j)\left(w_0+y_jw\prime_0+\sum_{i=1}^{\frac{1}{2}M}c_i\chi_i^2(y_j)+\sum_{i=1}^{\frac{1}{2}M}d_i\phi_i^2(y_j)\right)=f(y_j)+\frac{y_j}{M}\sum_{k=1}^{M}K(y_j,\tau_k)$$
$$\left(w_0+\tau_kw\prime_0+\sum_{i=1}^{\frac{1}{2}M}c_i\chi_i^2(\tau_k)+\sum_{i=1}^{\frac{1}{2}M}d_i\phi_i^2(\tau_k)\right),j=1,2,\ldots,M. \tag{70}$$

Simplifying Eq. (70), we get:

$$\sum_{i=1}^{\frac{1}{2}M} c_i\left(\chi_i(y_j)+h_1(y_j)\chi_i^1(y_j)+h(y_j)\chi_i^2(y_j)-\tfrac{y_j}{M}\sum_{k=1}^{M}K(y_j,\tau_k)\chi_i^2(\tau_k)\right)$$
$$+\sum_{i=1}^{\frac{1}{2}M} d_i\left(\phi_i(y_j)+h_1(y_j)\phi_i^1(y_j)+h(y_j)\phi_i^2(y_j)-\tfrac{y_j}{M}\sum_{k=1}^{M}K(y_j,\tau_k)\phi_i^2(\tau_k)\right)$$
$$=f(y_j)-h_1(y_j)w\prime_0-h(y_j)\left(w_0+y_jw\prime_0\right)+\tfrac{y_j}{M}\sum_{k=1}^{M}K(y_j,\tau_k)(w_0+\tau_kw\prime_0), j=1,2,\ldots,M. \tag{71}$$

Eq. (71) represents a linear system of M equations with M unknowns, *i.e.* $c_i, i=1,2,\ldots,\frac{1}{2}M$ and $d_i, i=1,2,\ldots,\frac{1}{2}M$. The system is solved for the unknowns, by making use of any linear algebra method. The approximate solution of the Volterra IDEs at collocation points $y_j, j=1,2,\ldots,M$ is then easily computed with the help of these coefficients and Eq. (65).

3.2.2.2. Nonlinear case. The first-order nonlinear Volterra IDEs is given bellow:

$$w\prime\prime(y)+h_1(y)\,w\prime(y)+h(y)\,w(y)$$
$$=f(y)+\int_0^y K(y,\tau,w(\tau))\mathrm{d}\tau, w(0)=w_0, w(1)=w_1. \tag{72}$$

Numerical integration yields the following equation:

$$w\prime\prime(y)+h_1(y)\,w\prime(y)+h(y)\,w(y)$$
$$=f(y)+\frac{y_j}{M}\sum_{k=1}^{M}K(y,\tau_k,w(\tau_k)). \tag{73}$$

In places of $w(y), w\prime(y)$ and $w\prime\prime(y)$, using their approximate linear Legendre wavelets expression and then discretizing the expression gives us:

$$Q_j\ \ (c_1,c_2,\ldots,c_{\frac{M}{2}},d_1,d_2,\ldots,d_{\frac{M}{2}})$$
$$=\sum_{i=1}^{\frac{1}{2}M}d_i\chi_i(y_j)+\sum_{i=1}^{\frac{1}{2}M}d_i\phi_i(y_j)+h_1(y_j)\left(w\prime_0+\sum_{i=1}^{\frac{1}{2}M}c_i\chi_i^1(y_j)+\sum_{i=1}^{\frac{1}{2}M}d_i\phi_i^1(y_j)\right)$$
$$+h(y_j)\left(w_0+y_jw\prime_0+\sum_{i=1}^{\frac{1}{2}M}c_i\chi_i^2(y_j)+\sum_{i=1}^{\frac{1}{2}M}d_i\phi_i^2(y_j)\right)$$
$$-\tfrac{y_j}{M}\sum_{k=1}^{M}K\left(y_j,\tau_k,w_0+\tau_kw\prime_0+\sum_{i=1}^{\frac{1}{2}M}c_i\chi_i^2(\tau_k)+\sum_{i=1}^{\frac{1}{2}M}d_i\phi_i^2(\tau_k)\right)-f(y_j)=0,$$
$$j=1,2,\ldots,M. \tag{74}$$

Eq. (74) is an $M\times M$ nonlinear system with M unknowns $c_i, i=1,2,\ldots,\frac{1}{2}M$ and $d_i, i=1,2,\ldots,\frac{1}{2}M$. Newton's, Broyden's or any other nonlinear technique can be utilized to obtain the solution. The unknown linear Legendre multi-wavelets coefficients can be obtained by solving the aforementioned nonlinear system. Utilizing these unknown coefficients of LMWs we can easily get the approximate solution at given collocation points.

The Jaccobian of the system given in Eq. (74) can be computed with the help of the following partial derivatives.

$$\frac{\partial Q_j}{\partial c_m}=\chi_m(y_j)+h_1(y_j)\chi_m^1(y_j)+h(y_j)\chi_m^2(y_j)$$
$$-\frac{y_j}{M}\sum_{k=1}^{M}\frac{\partial K}{\partial w}\chi_m^2(\tau_k),\ \ j=1,2,\ldots,M, \tag{75}$$

and

$$\frac{\partial Q_j}{\partial d_m}=\phi_m(y_j)+h_1(y_j)\phi_m^1(y_j)+h(y_j)\phi_m^2(y_j)$$
$$-\frac{y_j}{M}\sum_{k=1}^{M}\frac{\partial K}{\partial w}\phi_m^2(\tau_k),\ \ j=1,2,\ldots,M. \tag{76}$$

3.2.3. Fourth-order nonlinear Volterra IDEs

The fourth-order nonlinear Volterra IDEs is given by:

$$w^{iv}(y)+h_3(y)w\prime\prime\prime(y)+h_2(y)w\prime\prime(y)$$
$$=\int_0^y K(y,\tau,w(\tau),w\prime(\tau),w\prime\prime(\tau),w\prime\prime\prime(\tau),w^{iv}(\tau))\mathrm{d}\tau+f(y), \tag{77}$$

with boundary conditions

$$w(0)=v_0, w(1)=v_1, w\prime(0)=v\prime_0, w\prime(1)=v\prime_1. \tag{78}$$

Numerical integration yields the following equation:

$$w^{iv}(y)+h_3(y)w\prime\prime\prime(y)\ \ +h_2(y)w\prime\prime(y)+h_1(y)w\prime(y)+h(y)w(y)=f(y)$$
$$+\tfrac{y_j}{M}\sum_{k=1}^{M}K(y,\tau,w(\tau),w\prime(\tau),w\prime\prime(\tau),w\prime\prime\prime(\tau),w^{iv}(\tau)). \tag{79}$$

To obtained $w\prime\prime\prime(y), w\prime\prime(y), w\prime(y)$ and $w(y)$ integrate Eq. (22) and using the boundary conditions, we get:

$$w\prime\prime\prime(y)=\ \ 3\left(v\prime_1+v_0-\sum_{i=1}^{\frac{1}{2}M}c_ic_2'-\sum_{i=1}^{\frac{1}{2}M}d_id_2'+\sum_{i=1}^{\frac{1}{2}M}c_ic_3'+\sum_{i=1}^{\frac{1}{2}M}d_id_3'\right)$$
$$+\sum_{i=1}^{\frac{1}{2}M}c_i\chi_i^1(y)+\sum_{i=1}^{\frac{1}{2}M}d_i\phi_i^1(y), \tag{80}$$

$$w\prime\prime(y)=-\tfrac{3}{2}(v\prime_1+v_0)+\tfrac{1}{2}\left(\sum_{i=1}^{\frac{1}{2}M}c_ic_2'+\sum_{i=1}^{\frac{1}{2}M}d_id_2'\right)-\tfrac{3}{2}\left(\sum_{i=1}^{\frac{1}{2}M}c_ic_3'+\sum_{i=1}^{\frac{1}{2}M}d_id_3'\right)$$
$$+3y\left(v\prime_1+v_0-\sum_{i=1}^{\frac{1}{2}M}c_ic_2'-\sum_{i=1}^{\frac{1}{2}M}d_id_2'+\sum_{i=1}^{\frac{1}{2}M}c_ic_3'+\sum_{i=1}^{\frac{1}{2}M}d_id_3'\right)+\sum_{i=1}^{\frac{1}{2}M}a_i\chi_i^2(y)+\sum_{i=1}^{\frac{1}{2}M}d_i\phi_i^2(y), \tag{81}$$

$$w\prime(y)=v\prime_0+x\left(-\tfrac{3}{2}(v\prime_1+v_0)+\tfrac{1}{2}\left(\sum_{i=1}^{\frac{1}{2}M}c_ic_2'+\sum_{i=1}^{\frac{1}{2}M}d_id_2'\right)-\tfrac{3}{2}\left(\sum_{i=1}^{\frac{1}{2}M}c_ic_3'+\sum_{i=1}^{\frac{1}{2}M}d_id_3'\right)\right)$$
$$+\tfrac{3y^2}{2}\left(v\prime_1+v_0-\sum_{i=1}^{\frac{1}{2}M}c_ic_2'-\sum_{i=1}^{\frac{1}{2}M}d_id_2'+\sum_{i=1}^{\frac{1}{2}M}c_ic_3'+\sum_{i=1}^{\frac{1}{2}M}d_id_3'\right)$$
$$+\sum_{i=1}^{\frac{1}{2}M}c_i\chi_i^3(y)+\sum_{i=1}^{\frac{1}{2}M}d_i\phi_i^3(y), \tag{82}$$

and

$$w(y)=v_0+yv\prime_0+\tfrac{y^2}{2}\left(-\tfrac{3}{2}(v\prime_1+v_0)+\tfrac{1}{2}\left(\sum_{i=1}^{\frac{1}{2}M}c_ic_2'+\sum_{i=1}^{\frac{1}{2}M}d_id_2'\right)\right.$$
$$\left.-\tfrac{3}{2}\left(\sum_{i=1}^{\frac{1}{2}M}c_ic_3'+\sum_{i=1}^{\frac{1}{2}M}d_id_3'\right)\right)+\tfrac{y^3}{2}\left(v\prime_1+v_0-\sum_{i=1}^{\frac{1}{2}M}c_ic_2'-\sum_{i=1}^{\frac{1}{2}M}d_id_2'+\sum_{i=1}^{\frac{1}{2}M}c_ic_3'+\sum_{i=1}^{\frac{1}{2}M}d_id_3'\right)$$
$$+\sum_{i=1}^{\frac{1}{2}M}c_i\chi_i^4(y)+\sum_{i=1}^{\frac{1}{2}M}d_i\phi_i^4(y). \tag{83}$$

The rest of the procedure is similar as discussed in the previous cases.

4. Examples and discussion

This section is mainly concerned with the accuracy, efficiency and applications of the presented technique. Both linear and nonlinear types of model equations are used here to test the performace of the proposed method, *i.e.* first-order linear Fredholm IDEs, second-order linear Fredholm IDEs, first-order nonlinear Fredholm IDEs, first-order linear Volterra IDEs, second-order linear Volterra IDEs, nonlinear Volterra IDEs of the first-order, nonlinear first-order Fredholm–Volterra IDEs and second-order Volterra–Fredholm IDEs with singularity in the derivative are used for the testing. The notations $\mathbf{R}_c(M)$ and $\mathbf{E}_c(M)$ are used for computational convergence rates and maximum absolute errors at M collocation points (CPs). The following formula is used to calculate the experimental convergence rate

$$\mathbf{R}_c(M) = \frac{\mathbf{Log}\left[\frac{\mathbf{E}_c(\frac{1}{2}M)}{\mathbf{E}_c(M)}\right]}{\mathbf{Log}(\mathbf{2})}, \tag{84}$$

Broyden's technique is a useful option for the nonlinear case [23]. The initial value is set to zero and the computation is stopped when the convergence of 10^{-5} is reached.

The comparison of the results of the novel technique and HWCM have also been done [16] at Gauss Points (GPs) [17] defined by:

$$G_i = \left(\frac{3-\sqrt{3}}{6} + \frac{i-1}{2}\right)h, G_{i+1} = \left(\frac{3+\sqrt{3}}{6} + \frac{i-1}{2}\right)h,\ i = 1, 3, \ldots, N-1. \tag{85}$$

Test Problem 1. The first-order linear Fredholm IDEs[9] given by:

$$w\prime(y) = w(y) + \frac{1}{y+1} - \frac{1}{2}y - \log(y+1) + \frac{1}{(\log(2))^2}\int_0^1 \frac{y}{\tau+1} w(\tau)\mathrm{d}\tau, \tag{86}$$

$w(0) = 0.$

The exact answer of the problem is

$w(y) = \log(1+y).$

The Fig. 1 depicts the comparison of approximate solution with the exact solution for $M = 16$ number of collocation points. The figure clearly shows that the approximate solutions at the CPs are in close proximity to the exact solutions at the corresponding collocation points for a mere number of $M = 16$ of CPs.

Test Problem 2. Consider the second-order linear Fredholm IDEs [5]:

$$w\prime\prime(y) - \int_0^1 e^{y\tau} w(\tau)\,\mathrm{d}\tau = f(y), \tag{87}$$

with boundary conditions $w(0) = 0,\ w(1) = 0$, and

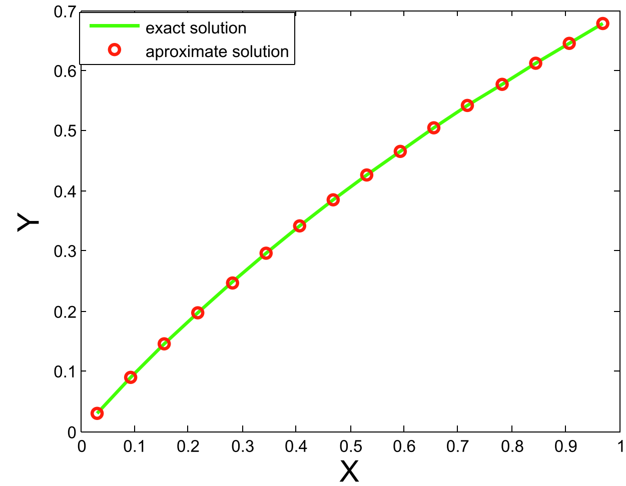

Fig. 1 Results of exact and approximate solution ($M = 16$) for Test Problem 1.

$$f(y) = \frac{2y^3 + (y-2)e^{y+y+2}}{y^3}.$$

Whereas, the exact solution is:

$w(y) = y^2 - y$

This is a second-order linear Fredholm IDE. The novel numerical technique is applied to this model equation. The $\mathbf{E}_c(M)$ and $\mathbf{R}_c(M)$ for distinct number of CPs are listed in Table 1. We did the comparison of the obtained approximate results with the Multi-scale Galerkin technique [5] and are shown in the aforementioned table. The comparison shows that the newly proposed numerical technique has more better approximation to the exact solution than the Multi-scale Galerkin method [5]. The exact and approximate results are also compared graphically and are demonstrated in the Fig. 2, for $M = 16$ number of CPs. On the whole, the approximate solution catch the exact solution very well.

Test Problem 3. Let us take the subsequent the first-order nonlinear Fredholm IDEs [16]:

$$w\prime(y) = 1 - \frac{1}{3}y^3 + \int_0^1 y^3 w(\tau)^2\,\mathrm{d}\tau, \quad w(0) = 0, \tag{88}$$

with exact solution:

$$w(y) = y. \tag{89}$$

This is a first order nonlinear Fredholm IDEs. The $\mathbf{E}_c(M)$ for different number of CPs are compared with the Haar wavelets collocation method [16] and the comparability is demonstrated in Fig. 3. The resulted approximate soltuion of the novel technique is compared with the Haar wavelets collocation method [16] is clearly seen from this figure. From the comparability of solutions it can be seen that the novel technique has much better accuracy than Haar wavelet method. Further, The decrease in $\mathbf{E}_c(M)$ to order 10^{-8} shows that the novel technique demonstrates equally good performance for nonlinear Fredholm problems too.

Table 1 The Comparison of $\mathbf{E}_c(M)$ of the newly proposed technique with Multi-scale Galerkin method [5] and $\mathbf{R}_c(M)$ of the proposed technique for Test Problem 2.

Newly proposed technique			Multi-scale Galerkin method [5].	
M	$\mathbf{E}_c(M)$	$\mathbf{R}_c(M)$	M	$\mathbf{E}_c(M)$
4	7.5214×10^{-4}	–	–	–
8	1.9596×10^{-4}	1.9404	15	6.5606×10^{-4}
16	4.9321×10^{-5}	1.9903	31	1.6398×10^{-4}
32	1.2330×10^{-5}	2.0000	63	4.0991×10^{-5}
64	3.0843×10^{-6}	1.9991	127	1.0248×10^{-5}
128	7.7111×10^{-7}	1.9999	255	2.5620×10^{-6}
256	1.9227×10^{-7}	1.9999	511	6.4105×10^{-7}

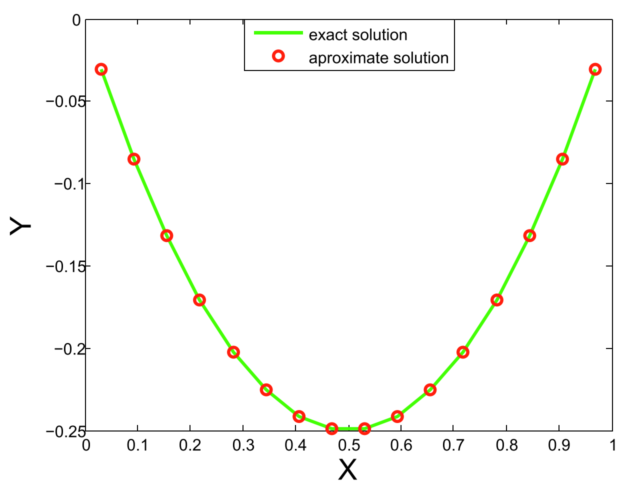

Fig. 2 Comparability of the exact and estimated results ($M=16$) for Test Problem 2.

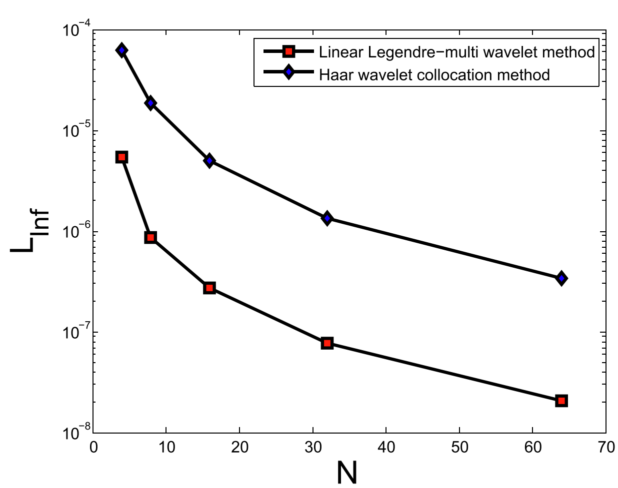

Fig. 3 Comparison of the proposed technique and Haar wavelets collocation method [16] for Test Problem 3 interms of maximum absolute errors.

Test Problem 4. Let us consider the first-order linear Volterra IDEs [20]:

$$w\prime(y) = 1 - \int_0^y w(\tau)\,d\tau,\ 0 \leqslant y \leq 1, \tag{90}$$

$$w(0) = 0. \tag{91}$$

The exact solution is listed as under:

$$w(y) = \sin y. \tag{92}$$

Table 2, shows the $\mathbf{E}_c(M)$ of the newly developed numerical technique for both distinct numbers of Collocatin points and Gauss points. It can be easily observed in the table that the accuracy of the newly proposed technique from the decrease of at gauss points is better than the CPs. Better accuracy of the novel technique can be observed from the decrease of $\mathbf{E}_c(M)$ to order 10^{-7} for just $M = 256$ numbers of collocatin points. Moreover, the technique performs better as we increase the number of CPs and GPs.

Test Problem 5. The subsequent is second-order linear Volterra IDEs:

$$w\prime\prime(y) = y + \int_0^y (y-\tau)\,w(\tau)\,d\tau. \tag{93}$$

with the following initial conditions and exact solution

$$w(0) = 0,$$
$$w\prime(0) = 1,$$

and

Table 2 The $\mathbf{E}_c(M)$ and $\mathbf{R}_c(M)$ of the proposed technique for Test Problem 4.

M	$\mathbf{E}_c(M)$ at CPs	$\mathbf{E}_c(M)$ at GPs	$\mathbf{R}_c(M)$
4	2.1000×10^{-3}	1.0000×10^{-3}	–
8	4.7295×10^{-4}	1.2878×10^{-4}	2.1506
16	1.0913×10^{-4}	3.6102×10^{-5}	2.1156
32	2.6248×10^{-5}	9.5001×10^{-6}	2.0557
64	6.4188×10^{-6}	2.4329×10^{-6}	2.0318
128	1.5861×10^{-6}	6.1533×10^{-7}	2.0168
256	3.9422×10^{-7}	1.5471×10^{-7}	2.0084

Table 3 Numerical results and comparabilty of $\mathbf{E}_c(M)$ of newly proposed method with HWC method [16] for Problem 5.

Newly proposed technique			Haar wavelets collocation method [16]	
M	$\mathbf{E}_c(M)$ at Cps	$\mathbf{E}_c(M)$ at GPs	$\mathbf{E}_c(M)$ at CPs	$\mathbf{E}_c(M)$ at GPs
4	2.3000×10^{-4}	3.6100×10^{-5}	5.0000×10^{-3}	2.5000×10^{-3}
8	4.9000×10^{-5}	1.3200×10^{-6}	1.4200×10^{-3}	6.4400×10^{-4}
16	1.1589×10^{5}	3.4353×10^{-7}	3.5255×10^{-4}	1.6221×10^{-4}
32	2.9855×10^{-6}	9.4874×10^{-8}	9.1980×10^{-5}	4.1021×10^{-5}
64	7.2161×10^{-7}	2.4149×10^{-8}	2.3121×10^{-5}	1.0021×10^{-5}
128	1.8791×10^{-7}	6.2354×10^{-9}	5.8132×10^{-6}	2.6111×10^{-6}
256	4.5560×10^{-8}	1.5634×10^{-9}	1.4866×10^{-6}	6.5877×10^{-7}

$w(y) = \sinh(y).$

In this problem, the novel method is used to solve a linear Volterra IDE of second-order. The comparison of the numerical results of this problem with Haar wavelets collocation method [16] and the comparability of $\mathbf{E}_c(M)$ for CPs as well as GPs are listed in the Table 3. The comparabilty demonstrates the accuracy of the novel technique is superior than the Haar wavelets collocation method [16] as we increase the numbers of CPs. The incredible performnce of the novel method is witnessed by observing fall of $\mathbf{E}_c(M)$ to order 10^{-9} for just $M = 256$ number of GPs.

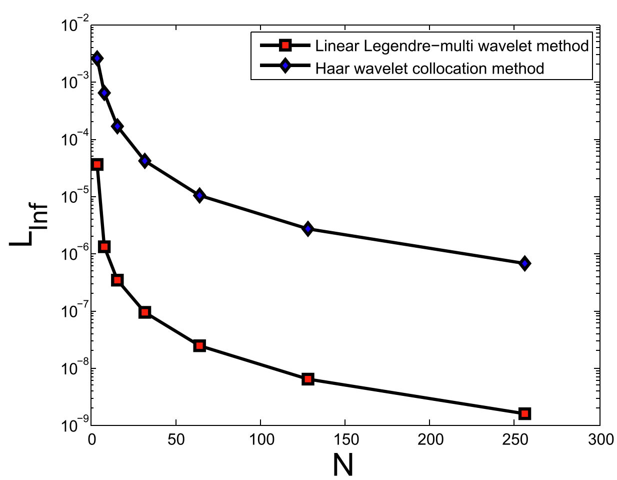

Fig. 4 Comparison of the maximum absolute error of proposed method with HWCM (at GPs) for Test Problem 5.

Also, the graphical comparability the newly proposed technique with Haar wavelets collocation method [16] for $M = 16$ number of Gauss points is demonstared in Fig. 4.

Test Problem 6. Consider the following nonlinear first-order Volterra IDE [9]:

$$w\prime(y) = 2y - \frac{1}{2}\sin(y^4) + \int_0^y y^2\tau\cos y^2 w(\tau)\,d\tau,$$
$$w(0) = 0,\ 0 < y < 1, \tag{94}$$

with the following exact solution:

$w(y) = y^2.$

The results of the novel technique and Meshless method [9] are compared for $\mathbf{E}_c(M)$. The $\mathbf{E}_c(M), \mathbf{R}_c(M)$ and the total iterations of the novel technique are listed in Table 4. Clearly, the aforementioned table shows that the newly proposed technique has much better accuracy than Meshless method [9]. The number of iterations taken by the Broyden's method for this test problem for distinct numbers of CPs is same and is equal to 4. This establishes that the novel technique is quite efficient for nonlinear problems as well. Moreover, the comparability between exact and estimated results for $M = 16$ number of CPs is shown in Fig. 5.

Test Problem 7. Consider the following fourth-order nonlinear Volterra IDEs [16]:

$$w^{iv}(y) = 1 + \int_0^y e^{-\tau} w^2(\tau)\,d\tau, \quad 0 < y < 1, \tag{95}$$

with boundary conditions:

Table 4 Comparability of $\mathbf{E}_c(M)$ of the novel technique with Meshless method [9] and $\mathbf{R}_c(M)$ of the novel technique for Test Problem 6.

Newly proposed technique				Meshless method [9]	
M	$\mathbf{E}_c(M)$	$\mathbf{E}_c(M)$	No of iterations	M	$\mathbf{E}_c(M)$
4	1.2094×10^{-4}	–	4	5	5.8400×10^{-3}
8	5.2711×10^{-5}	1.1981	4	9	1.7500×10^{-3}
16	1.9107×10^{-5}	1.4640	4	17	4.8800×10^{-4}
32	5.8377×10^{-6}	1.7106	4	33	1.3000×10^{-4}
64	1.6122×10^{-6}	1.8563	4	65	3.2100×10^{-5}
128	4.2328×10^{-7}	1.9293	4	129	8.1900×10^{-6}

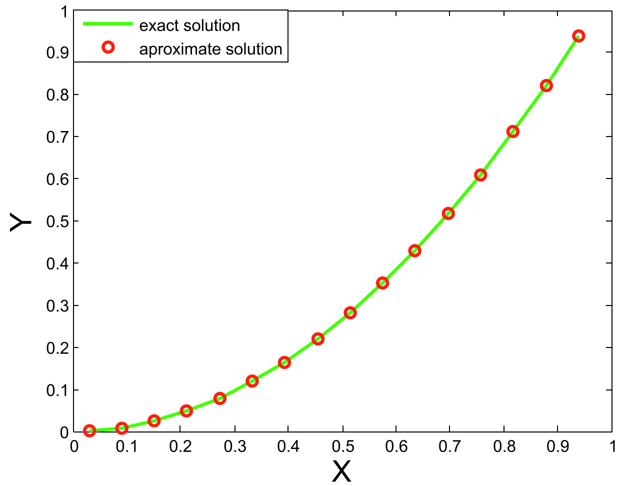

Fig. 5 Comparability of exact and estimated solutions ($M = 16$) for Test Problem 6.

$$w(0) = 1, \quad w\prime(0) = 1, \quad w(1) = e, \quad w\prime(1) = e. \tag{96}$$

The exact solution for this problem is given by:

$$w(y) = y^2. \tag{97}$$

Table 5 Comparability of $\mathbf{E}_c(M)$ of newly proposed technique with Haar wavelets collocation method [16] and $\mathbf{R}_c(M)$ of newly presented technique for Test Problem 7.

Newly proposed technique			Haar wavelets collocation method [16]
M	$\mathbf{E}_c(M)$	$\mathbf{R}_c(M)$	$\mathbf{E}_c(M)$
4	1.0533×10^{-5}	–	3.8300×10^{-5}
8	3.2148×10^{-6}	1.7121	1.0100×10^{-5}
16	8.1875×10^{-7}	1.9732	2.5600×10^{-6}
32	2.0487×10^{-7}	1.9987	6.4100×10^{-7}
64	5.1208×10^{-8}	2.0002	1.6000×10^{-7}

Table 5, lists the $\mathbf{E}_c(M)$ of the novel technique for different numbers of CPs. The table demonstrates the comparability of $\mathbf{E}_c(M)$ of the newly proposed technique with Haar wavelets collocation method [16] for various number of CPs. Table 5 also lists the $\mathbf{R}_c(M)$ of the novel technique which approach to 2. The much better accuracy of the newly proposed technique is noticeable from this table.

Test Problem 8. Consider the subsequent nonlinear first-order Fredholm–Volterra IDE [16]:

$$w\prime(y) + w(y) = f(y) + \frac{1}{4}\int_0^1 \tau w^3(\tau)\,\mathrm{d}\tau - \frac{1}{2}\int_0^y y w^2(\tau)\,\mathrm{d}\tau,$$

$$w(0) = 0, \tag{98}$$

where

$$f(y) = \frac{1}{10}y^6 + y^2 + 2y - \frac{1}{32}, \tag{99}$$

with exact solution:

$$w(y) = y^2. \tag{100}$$

This is nonlinear first order Fredholm–Volterra IDE. The performance of the novel technique is also assessed on this model equation. The point wise comparability of $\mathbf{E}_c(M)$ of the novel technique with the Haar wavelets collocation method [16] are reported in Table 6. Here we presented the point wise $\mathbf{E}_c(M)$ of the newly proposed technique for ($M = 16$) and ($M = 32$) numbers of CPs. Clearly, we can see that the novel technique performs better to some extent than Haar wavelets collocation technique [16] in terms of accuracy. (See Table 7)

Test Problem 9. Consider the second-order Volterra–Fredholm IDE with singularity in the derivative [16] given bellow:

$$w\prime\prime(y) + \tfrac{1}{\sqrt{y}}w\prime(y) + \tfrac{1}{y}w(y) = g(y) - w^{11}(y) + e^{w^9(y)} + \tfrac{1}{\sin(w^2(y))+1} - \int_0^y (y+\tau)w(\tau)\mathrm{d}\tau - \int_0^1 \tau\, y\, w(\tau)\mathrm{d}\tau, 0 < x < 1, \tag{101}$$

taken the boundary constraints $w(0) = 0, w(1) = 0$. The $g(y)$ is as follows:

Table 6 Point wise comparability of $\mathbf{E}_c(M)$ of the novel method with Haar wavelets collocation method [16] for Problem 8.

y	Newly proposed technique (M = 16)	Haar wavelets collocation method [16] (M = 16)	Newly proposed technique (M = 32)	Haar wavelets collocation method [16] (M = 32)
0	0	0	0	0
0.1	2.88×10^{-5}	8.20×10^{-4}	7.19×10^{-6}	1.20×10^{-4}
0.2	5.48×10^{-5}	4.00×10^{-4}	1.37×10^{-5}	1.70×10^{-4}
0.3	7.83×10^{-5}	3.00×10^{-4}	1.95×10^{-5}	1.50×10^{-4}
0.4	9.95×10^{-5}	5.30×10^{-4}	2.48×10^{-5}	5.40×10^{-4}
0.5	1.18×10^{-4}	4.90×10^{-4}	2.96×10^{-5}	1.20×10^{-4}
0.6	1.34×10^{-4}	3.70×10^{-4}	3.36×10^{-5}	1.40×10^{-5}
0.7	1.47×10^{-4}	2.20×10^{-5}	3.69×10^{-5}	7.30×10^{-4}
0.8	1.55×10^{-4}	1.00×10^{-4}	3.88×10^{-5}	5.20×10^{-4}
0.9	1.55×10^{-4}	1.20×10^{-4}	3.88×10^{-5}	4.80×10^{-4}
1.0	1.42×10^{-4}	9.10×10^{-4}	3.35×10^{-5}	2.20×10^{-4}

Table 7 The $\mathbf{E}_c(M)$ of the novel method for Problem 9.

M	$\mathbf{E}_c(M)\ w(y)$	$\mathbf{E}_c(M)\ w\prime(y)$
4	$2.3000\ \times 10^{-3}$	$1.0900\ \times 10^{-2}$
8	$7.3699\ \times 10^{-4}$	$3.3000\ \times 10^{-3}$
16	$1.9351\ \times 10^{-4}$	$9.2241\ \times 10^{-4}$
32	$4.1454\ \times 10^{-5}$	$2.1440\ \times 10^{-4}$
64	$2.3227\ \times 10^{-6}$	$2.3449\ \times 10^{-5}$

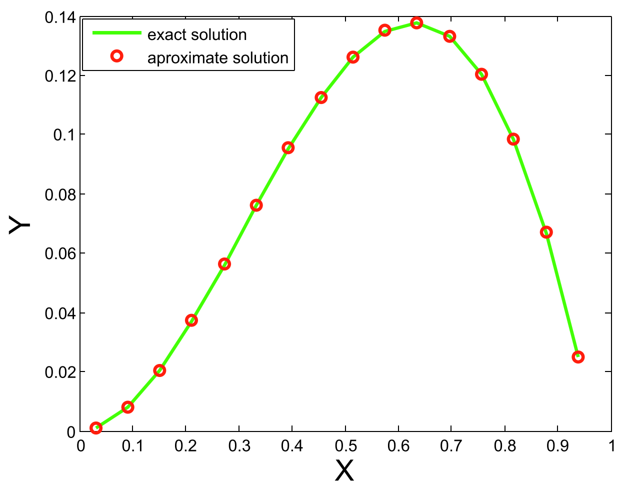

Fig. 6 Comparability of exact and estimated solution ($M = 16$) for Test Problem 9.

$$f(y) = \frac{1}{\sqrt{y}}((2\sqrt{y} - 4y\sqrt{y} - y^2 + y)\cos y + (1 + y^2\sqrt{y} - 2y - \sqrt{y} - 2y\sqrt{y})\sin y) + 2(y^3 - y^2 - 4y + 1)\cos y + 2(y-1) + (6 + 3y - 5y^2)\sin y - (4\cos 1 - 5\sin 1 + 2)y - \frac{1}{\sin(((y-y^2)\sin y)^2)+1} - e^{(((y^2-y)\sin y)^2)^9} + (((y-y^2)\sin y)^2)^{11}. \quad (102)$$

Whereas, the exact solution is:

$$w(y) = (y - y^2)\sin y.$$

Fig. 6, demonstrated the comparability of exact and estimated results for distinct numbers of CPs. The singularity of the aforementioned model equation occur at $y = 0$. The estimated results of the newly proposed technique are quite good for both w and w'. The novel technique dealt with the singularity at $y = 0$ without special treatment in the algorithm by utilizing the property of linear Legendre multi-wavelets. When the CPs are constructed, the Legendre multi-wavelets not utilize the ends points of the interval into account.

5. Conclusion

A collocation method based on linear Legendre multi-wavelets is introduced for the numerical solution of both linear and nonlinear Fredholm, Volterra and Volterra–Fredholm IDEs. The performance of the novel numerical technique is examined with the help of several model equations and the estimated results show that efficiency and accuracy of the presented technique is better than Multi-scale Galerkin method, Haar wavelets collocation method and Meshless method. The significant quality of the novel technique is its applicability to three different types of linear and also nonlinear integro-differential equations with very small modification.

Declaration of Competing Interest

The authors declare that they have no known competing financial interests or personal relationships that could have appeared to influence the work reported in this paper.

References

[1] Aziz, I. and Khan, I., 2017. Numerical Solution of Partial Integrodifferential Equations of Diffusion Type. Mathematical Problems in Engineering, 2017.
[2] Syam, M.I., Al-Mdallal, Q.M. and Anwar, M.N., 2015. An efficient numerical algorithm for solving fractional higher-order nonlinear integrodifferential equations. In Abstract and Applied Analysis (Vol. 2015). Hindawi.
[3] Q.M. Al-Mdallal, Boundary value problems for nonlinear fractional integro-differential equations: theoretical and numerical results, Advances in Difference Equations 2012 (1) (2012) 18.
[4] Q.M. Al-Mdallal, Monotone iterative sequences for nonlinear integro-differential equations of second order, Nonlinear Analysis: Real World Applications 12 (6) (2011) 3665–3673.
[5] J. Chen, Y. Huang, H. Rong, T. Wu, T. Zeng, A multiscale Galerkin method for second-order boundary value problems of Fredholm integro-differential equation, J. Comput. Appl. Math. 290 (2015) 633–640.
[6] H. Danfu, S. Xufeng, Numerical solution of integro-differential equations by using CAS wavelet operational matrix of integration, Applied mathematics and computation 194 (2) (2007) 460–466.
[7] P. Darania, A. Ebadian, A method for the numerical solution of the integro-differential equations, Appl. Math. Comput. 188 (1) (2007) 657–668.
[8] A. Akyüz-Daşcıoğlu, M. Sezer, Chebyshev polynomial solutions of systems of higher-order linear Fredholm-Volterra integro-differential equations, J. Franklin Inst. 342 (6) (2005) 688–701.
[9] M. Dehghan, R. Salehi, The numerical solution of the non-linear integro-differential equations based on the meshless method, J. Comput. Appl. Math. 236 (9) (2012) 2367–2377.
[10] S.M. Hosseini, S. Shahmorad, Numerical solution of a class of integro-differential equations by the Tau method with an error estimation, Appl. Math. Comput. 136 (2–3) (2003) 559–570.
[11] M.T. Kajani, M. Ghasemi, E. Babolian, Comparison between the homotopy perturbation method and the sine-cosine wavelet method for solving linear integro-differential equations, Computers & Mathematics with Applications 54 (7–8) (2007) 1162–1168.
[12] M.T. Kajani, M. Ghasemi, E. Babolian, Numerical solution of linear integro-differential equation by using sine-cosine wavelets, Appl. Math. Comput. 180 (2) (2006) 569–574.
[13] K. Maleknejad, F. Mirzaee, Numerical solution of integro-differential equations by using rationalized Haar functions method, Kybernetes (2006).
[14] M.T. Rashed, Numerical solution of functional differential, integral and integro-differential equations, Appl. Math. Comput. 156 (2) (2004) 485–492.
[15] V.K. Singh, O.P. Singh, R.K. Pandey, Numerical evaluation of the Hankel transform by using linear Legendre multi-wavelets, Comput. Phys. Commun. 179 (6) (2008) 424–429.
[16] I. Aziz, A.S. Al-Fhaid, An improved method based on Haar wavelets for numerical solution of nonlinear integral and integro-differential equations of first and higher orders,

Journal of computational and applied mathematics 260 (2014) 449–469.
[17] I. Aziz, F. Haq, A comparative study of numerical integration based on Haar wavelets and hybrid functions, Computers & Mathematics with Applications 59 (6) (2010) 2026–2036.
[18] S. Yalçinbaş, M. Sezer, The approximate solution of high-order linear Volterra-Fredholm integro-differential equations in terms of Taylor polynomials, Appl. Math. Comput. 112 (2–3) (2000) 291–308.
[19] E. Yusufoğlu, Improved homotopy perturbation method for solving Fredholm type integro-differential equations, Chaos, Solitons & Fractals 41 (1) (2009) 28–37.
[20] S. Yuzbapy, N. Pahin, M. Sezer, Bessel polynomial solutions of high-order linear Volterra integro-differential equations, Computers & Mathematics with Applications 62 (4) (2011) 1940–1956.
[21] S. Yuzbapy, N. Pahin, A. Yildirim, A collocation approach for solving high-order linear Fredholm-Volterra integro-differential equations, Mathematical and Computer Modelling 55 (3–4) (2012) 547–563.
[22] J. Zhao, R.M. Corless, Compact finite difference method for integro-differential equations, Applied mathematics and computation 177 (1) (2006) 271–288.
[23] Burden, R.H. and Faires, J.D., 2011. Numerical Analysis Ninth Edition. Brooks/Cole 20 Channel Center Street Boston MA 02210 USA.
[24] Asif, M. and Haider, N. and Mdallal, Q.A. and Khan, I., 2020. A Haar wavelet collocation approach for solving one and two-dimensional second-order linear and nonlinear hyperbolic telegraph equations. Numerical Methods for Partial Differential Equations, (34), doi: 10.1002/num.22512.
[25] Amin, R. and Shah, K. and Asif, M. and Khan, I., 2020. Efficient numerical technique for solution of delay Volterra-Fredholm integral equations using Haar wavelet. Heliyon, (6), p-2023-2034, e05108.
[26] I. Aziz, M. Asif, S. Islam, Haar wavelet collocation method for three-dimensional elliptic partial differential equations, Comput. Math. Appl. 34 (2017) 2023–2034.
[27] Dehestani, H. and Ordokhani, Y. and Razzaghi, M., 2019. On the applicability of Genocchi wavelet method for different kinds of fractional-order differential equations with delay. Numerical linear Algebra with Applications, (26), p-2259.
[28] H. Dehestania, Y. Ordokhania, M. Razzaghib, Combination of Lucas wavelets with Legendre-Gauss quadrature for fractional Fredholm-Volterra integro-differential equations, J. Comput. Appl. Math. 382 (2021) 113070.
[29] H. Dehestania, Y. Ordokhania, M. Razzaghib, Fractional-order Bessel functions with various applications, Applications of Mathematics 64 (2019) 637–662.
[30] Dehestania, H. and Ordokhania, Y. and Razzaghib M., 2020. Pseudo-operational matrix method for the solution of variable-order fractional partial integro-differential equations. Engineering with Computers, (64), doi: 10.1007/s00366-019-00912-z.
[31] E. Hashemizadeh, S. Rahbar, The Application of Legendre Multiwavelet Functions in Image Compression. Journal of Modern Applied, Statistical Methods 15 (2016) 1–17.
[32] X. Xiaoyong, X. Xu, Legendre wavelets direct method for the numerical solution of time-fractional order telegraph equations, Mediterr. J. Math. 15 (2018) 1–13.
[33] X. Xiaoyong, X. Xu, A semi-discrete scheme for solving fourth-order partial integro-differential equation with a weakly singular kernel using Legendre wavelets method, Computational and Applied Mathematics 37 (2017) 4145–4168.
[34] X. Xiaoyong, X. Xu, Legendre wavelets method for approximate solution of fractional-order differential equations under multi-point boundary conditions, International Journal of Computer Mathematics 95 (2017) 998–1014.